

# The Time-settlement Behaviour of Rafts of Finite Flexibility

J.C. SMALL

Lecturer, School of Civil and Mining Engineering, University of Sydney

**SUMMARY** A method is presented for computing the time-settlement behaviour of circular rafts of finite flexibility, resting on soil layers of finite depth. Results are presented for the time-settlement behaviour of rafts on soil layers of various depths, as well as for the development of moment in the raft with time.

## 1. INTRODUCTION

Theoretical predictions of the rate of settlement of foundations have undergone much development since Terzaghi published his one dimensional consolidation theory in 1925. Solutions were extended to three-dimensional loadings applied to porous elastic media (McNamee and Gibson (1960), Gibson and McNamee (1963), Gibson et al (1970) and Booker (1974)) and work was done to determine the elastic parameters required for such theories from laboratory testing. (Davis and Poulos (1963,1972)).

However in all of the solutions previously mentioned, it has been assumed that the loading applied to the soil was a uniformly distributed load, and no attempt was made to include the effects of soil-structure interaction. By including the structure which is applying the loading to the soil, loadings quite different to the uniform load case arise over the surface of contact between structure and soil.

Investigators have previously obtained solutions for raft foundations on an elastic soil (Borowicka (1936), Habel (1937), Holmberg (1946), Brown (1969 a,b)) but these are useful only in predicting short term (undrained) or long term (drained) behaviour. They cannot be used to predict the period of time necessary for such raft foundations to develop their maximum deflections and moments, and whether the maximum moments and differential deflections are exceeded during consolidation.

In this paper a method is presented for obtaining the time-settlement behaviour of a circular raft of finite flexibility on a soil layer of finite depth, where the soil is considered to be a homogeneous, linearly elastic, porous medium. The solution is obtained by calculating the response of both the soil and the raft to a general reaction distribution and then determining the precise form of the distribution by invoking displacement compatibility at the raft-soil interface.

## 2. THEORY

The raft-soil system is shown schematically in Figure 1(a) where the circular raft of radius  $a$  and thickness  $t_r$  has a Young's modulus  $E_r$  and Poisson's ratio  $\nu_r$ . The loading is assumed to be a uniform time dependent loading  $q_A(t)$  applied to the surface of the raft, although the theory is easily extended to accommodate other loading distributions such as ring loads. It is also assumed that the soil upon which the raft is

resting is a porous elastic medium which occupies the region  $0 \leq z \leq h$  and having a Young's modulus  $E_s$ , Poisson's ratio  $\nu_s$ , and permeability  $k_s$ .

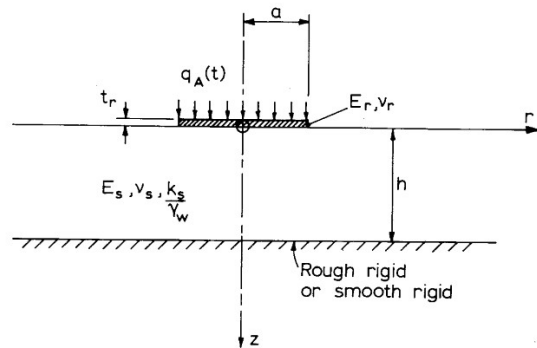


Fig. 1a Raft on Finite Layer

Two different boundary conditions were considered for the base  $z = h$  of the layer of soil; namely a rough-rigid impermeable base (i.e. vertical  $w$  and radial  $u$  displacements are zero, and pore pressure gradient  $\partial p / \partial z$  is zero) or a smooth rigid base (i.e. vertical displacement  $w$  and shear stress  $\sigma_{rz}$  are zero). The upper boundary of the soil is assumed to be free to drain across the entire surface (i.e.  $p = 0$  on  $z = 0$ ).

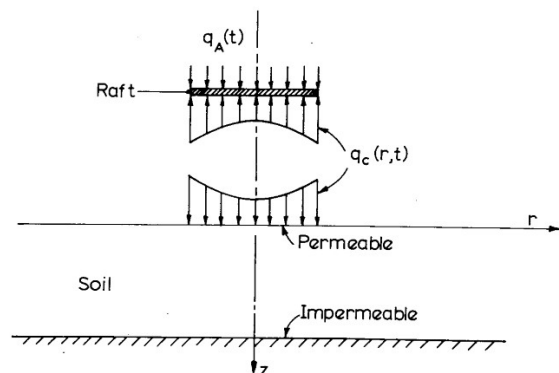


Fig. 1b Soil-Raft System

Figure 1(b) shows the raft and soil considered separately. The unknown contact stress  $q_c(r, t)$  (which is a function of both radius and time) between the raft and soil is unknown and must be determined. This may be done by assuming that the contact stress may be represented in the form suggested by Brown (1969b) i.e.:

$$q_c(r, t) = \sum_{n=1}^N F_n(t) \phi_n(r) \quad (1)$$

Where  $F_n(t)$  can be considered as generalized forces and

$$\begin{aligned} \phi_n &= (1 - (r/a)^2)^n \quad n = 0, 1, 2, \dots, N-1 \\ \phi_N &= (1 - (r/a)^2)^{-1/2} \end{aligned}$$

## 2.1 Analysis of Raft

It may be shown, using the theory of Timoshenko and Woinowsky-Krieger (1959), that the deflection of a centrally supported circular raft subjected to a ring load at radius  $r_0$  is given by the Green's function  $G(r, r_0)$  where

$$G(r, r_0) = \frac{1}{4D_r} \left[ r^2 \left( 1 + \ln \frac{r}{r_0} \right) + \frac{1}{2} \frac{(1-\nu_r) r^2 r_0^2}{(1+\nu_r) a^2} \right] \quad r_0 < r < a$$

$$G(r, r_0) = \frac{1}{4D_r} \left[ r^2 \left( 1 + \ln \frac{r_0}{r} \right) + \frac{1}{2} \frac{(1-\nu_r) r^2 r_0^2}{(1+\nu_r) a^2} \right] \quad 0 < r < r_0 \quad (2)$$

$D_r = E_r t_r / (12(1-\nu_r^2))$  is the flexural rigidity of the raft.

In the case where a uniform loading  $q_A(t)$  is applied to the raft, the net load acting is  $q_A(t) - q_c(r, t)$  and we may use (2) to calculate the deflection of the raft i.e.

$$w(r, t) = w_0(t) + \int_0^a G(r, r_0) [q_A(t) - q_c(r, t)] dr_0 \quad (3)$$

where  $w(r, t)$  is the vertical deflection of the raft at radius  $r$  and time  $t$  and  $w_0(t)$  is the as yet unknown central deflection of the raft.

It is now convenient to introduce the quantities  $\delta_m(t)$  defined as:

$$\delta_m(t) = \int_0^a r \phi_m(r) w(r, t) dr \quad (4)$$

These quantities arise from a consideration of the virtual work performed by the reaction distribution and are, to within a factor  $2\pi$ , the generalised deflections corresponding to the generalised forces  $F_n(t)$ . Compatibility of the soil-raft system may now be approximated by assuming that the generalised deflections of the raft are equal to those of the soil. The advantage of this approach over previous methods, (Brown 1979b) is that deflections do not have to be matched at specified points along the raft-soil interface.

If we combine (3) and (4) we obtain the flexibility relationship:

$$\delta_m(t) = \xi_m w_0(t) + \gamma_m(t) - \sum_{n=1}^N H_{mn} F_n(t) \quad (5)$$

where

$$\xi_m = \int_0^a r \phi_m(r) dr$$

$$H_{mn} = \int_0^a \int_0^a r r_0 G(r, r_0) \phi_m(r) \phi_n(r) dr dr_0$$

$$\begin{aligned} \gamma_m(t) &= \int_0^a \int_0^a r r_0 G(r, r_0) \phi_m(r) q_A(t) dr dr_0 \\ &= H_{m0} q_A(t) \end{aligned}$$

The coefficients  $H_{mn}$  are easily calculated by evaluating the double integral in the above expression. Values of  $H_{mn}$  are given by Booker and Small (1983).

## 2.2 Analysis of Soil

Using the theory of McNamee and Gibson (1960) it is shown in Appendix A that the deflection  $w$  of the surface  $z = 0$  of an elastic layer of soil subject to a loading  $q_c(r, t)$  on its upper surface is given by

$$\bar{w} = \frac{1}{2G} \int_0^\infty \alpha \rho(\alpha, s) \sum_{n=1}^N \bar{F}_n \phi_n(\alpha) J_0(\alpha r) d\alpha \quad (6)$$

where the superior bar denotes a Laplace transformation,  $G$  is the shear modulus of the soil and  $\phi(\alpha)$  is a function defined in Appendix A.

The term  $\rho(\alpha, s)$  is a function of the Hankel transform parameter  $\alpha$  and the Laplace transform parameter  $s$ . The value of  $\rho(\alpha, s)$  will depend on whether the base of the layer is rough or smooth and values are given for the two cases in Appendix A.

From the definition of  $\delta_m(t)$  given in (4) we may calculate the quantity  $\delta_m$  for the soil.

$$\delta_m = \sum_{n=1}^N F_n P_{mn} \quad (7)$$

$$\text{Where } P_{mn} = \int_0^\infty \frac{\alpha \rho(\alpha, s)}{2G} \phi_n(\alpha) \phi_m(\alpha) d\alpha$$

## 2.3 Force Balance Equation

We must also consider vertical force equilibrium for the raft. This leads to the force balance equation

$$\int_0^{2\pi} \int_0^a q_A(t) r dr d\theta -$$

$$\int_0^{2\pi} \int_0^a \sum_{n=1}^N F_n(t) \phi_n(r) r dr d\theta = 0 \quad (8)$$

which may be written:

$$\sum_{n=1}^N \xi_n F_n(t) = P_A(t)/2\pi$$

where  $P_A(t)$  is the total load applied to the plate at any time and  $\xi_n$  is as defined in (5).

### 3. ANALYSIS OF SOIL-RAFT SYSTEM

Equations (5), (7), (8) expressed in matrix form and written in Laplace transform space become

$$\begin{aligned} \delta &= \xi w_0 + \gamma - H F \\ \delta &= P F \\ T &= P / 2\pi \\ \xi F &= A \end{aligned} \quad (9)$$

The above equations may now be combined to give the final set of equations for the soil-raft system.

$$\begin{bmatrix} H + \bar{P} & -\xi \\ -\xi^T & 0 \end{bmatrix} \begin{bmatrix} \bar{F} \\ w_0 \end{bmatrix} = \begin{bmatrix} -\bar{\gamma} \\ -\bar{P}_A/2\pi \end{bmatrix} \quad (10)$$

By solving (10) we may obtain the solution for the Laplace transformation of the generalised forces  $\bar{F}$  and the central deflection of the raft  $w_0$ . To obtain the solution at any time  $t$  we must invert the Laplace transformations, and this may be done numerically using the numerical techniques of Talbot (1979). The matrix  $P$  may also be evaluated using numerical means such as Gaussian integration (see (7)).

Once the generalised force coefficients  $F_n(t)$  have been found, it is a simple matter to calculate moments and deflections in the raft using the theory of Timoshenko and Woinowsky-Krieger (1959).

### 4. EXAMPLES

As an illustration of the theory presented in the previous section, the problem of a circular raft on a consolidating layer of soil of finite depth was considered. It was assumed that the raft had a radius  $a$  and that the load  $q_A$  is applied at  $t = 0^+$  and thereafter held constant. The layer of soil was chosen to be of depth  $h$  such that  $h/a = 1$  and the Poisson's ratio of the soil was chosen to be  $\nu_s = 0$  with that of the raft to be  $\nu_r = 0.3$ .

Results are presented for two different boundary conditions at the base of the layer; those in Figure 2 for a rough-rigid base and those in Figure 3 for a smooth rigid base (see section 2). Plotted is the non-dimensional central deflection  $Gw(0,t)/q_A$  versus the time factor  $\tau$  where

$$\tau = ct/a^2 \quad (11)$$

and  $c$  is defined in Appendix A.

In each of the figures, results are presented for

various raft stiffnesses  $K = 0.1, 1.0, 10$ , where  $K$  is defined as:

$$K = \frac{E_r}{E_s} (1 - \nu_s^2) \cdot (t_r/a)^3 \quad (12)$$

(the quantities in this expression are defined in section 2).

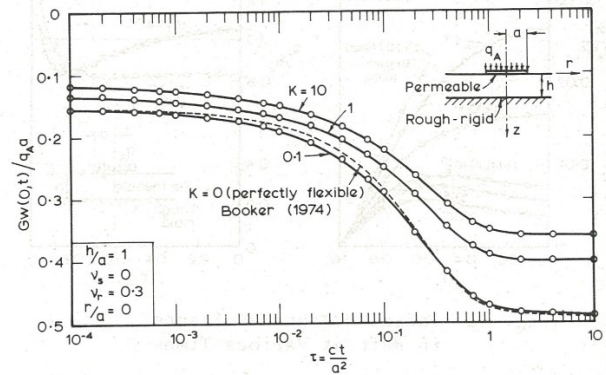


Fig. 2 Time-Deflection Behaviour of Circular Raft Rough Based Layer

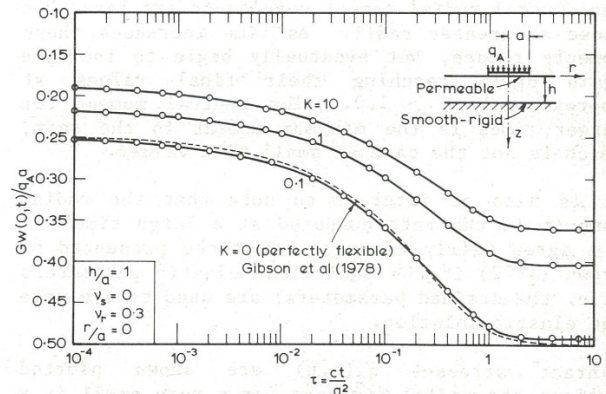


Fig. 3 Time-Deflection Behaviour of Circular Raft Smooth Based Layer

In each of Figures 2 and 3 the same general trends may be observed; that is the deflection of the raft decreases with increasing stiffness but that the rate at which consolidation proceeds is approximately the same. For very flexible rafts the time-deflection curves should be like those for a uniformly distributed load. In each of the Figures 2 and 3, the analytic solutions for a uniform loading have been plotted (Booker (1974) rough base; Gibson et al (1970) smooth base). It may be noticed that for a raft of stiffness  $K = 0.1$ , the deflection of the central point is initially slightly less than for the uniform loading, but becomes slightly larger at intermediate times before once again becoming smaller at large times. This trend is evident for both rough and smooth bases.

It is also possible to compute radial  $M_r$  and tangential  $M_\theta$  moment resultants (i.e. moment per unit length) in the raft at any time during the consolidation process. An example of this is given in Figure 4(a). In this figure results are presented for the radial moments in the raft at various nondimensional times  $\tau$ . The particular



problem chosen was as shown in the inset to Figure 4(b) where the base of the layer was taken as being perfectly rough and the layer depth such that  $h/a = 0.5$ . Loading is a uniform load  $q_A$  applied at time  $t = 0^+$  and thereafter held constant. All other parameters chosen for the problem are indicated on Figure 4(a).

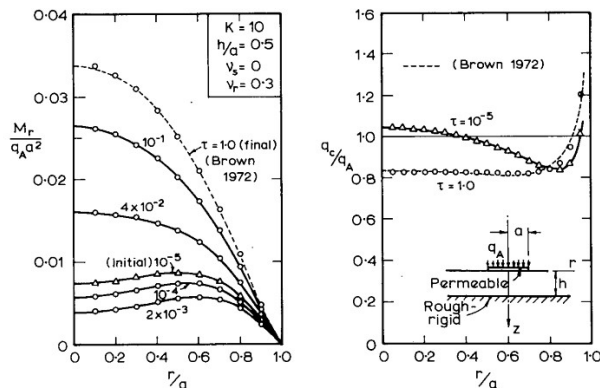


Fig. 4a Radial Moment Resultants in Raft at Various Times

Fig. 4b Initial and Final Contact Stress Distributions

At very small times ( $\tau = 10^{-5}$ ) it may be seen that the central radial moment resultants are less than those at greater radii. As time increases these moments reduce, but eventually begin to increase again until reaching their final values at approximately  $\tau = 1.0$ . The central moment for larger times is the maximum moment in the raft, which is not the case at small time values.

It is also of interest to note that the radial moments in the raft computed at a large time  $\tau = 1.0$  agree fairly closely with those presented by Brown (1972) if the equivalent elastic parameters (i.e. the drained parameters) are used to evaluate the elastic solution.

Contact stresses  $q_c(r, t)$  are shown plotted against the radial distance for a very small ( $\tau = 10^{-5}$ ) and a large time ( $\tau = 1$ ). Substantial changes occur in the contact stress distribution as consolidation proceeds with these stresses tending to decrease across the central portion of the raft, and increase at the edge. As for the moments, the contact stresses agree with the solutions of Brown (1972) for large times if the drained elastic parameters are used to evaluate Brown's elastic solution.

The reason for decrease in moment occurring in the plate as consolidation occurs is that the high pore pressures which are initially generated at the edge of the raft rapidly dissipate, causing the edge of the raft to deflect more rapidly than the central portion. This causes a reduction in differential deflection in the raft; hence a decrease in moment. Differential deflections increase again at larger times and as a consequence moments also increase.

Plots of radial moment resultant versus time and differential deflection versus time are shown in Figures 5 and 6 respectively. These plots demonstrate the initial decrease in radial moment  $M$  and differential deflection  $\Delta$  in the raft ( $\Delta = w(a, t) - w(0, t)$ ). The particular plots presented are for a problem similar to the previous one except that the raft is of flexibility  $K = 1.0$  and the soil has a Poisson's ratio of  $v_s = 0.2$ .

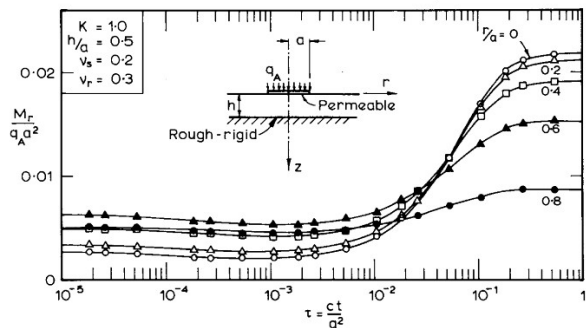


Fig. 5 Variation of Radial Moment in Raft With Time

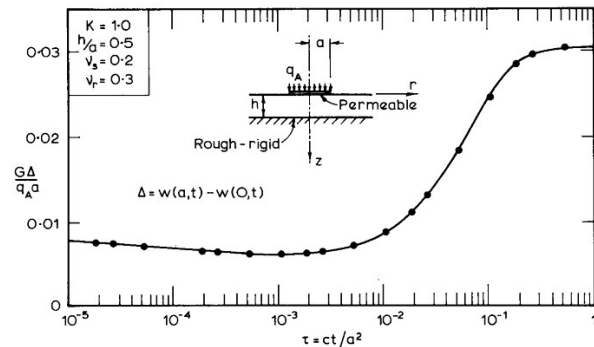


Fig. 6 Variation of Differential Deflection in Raft With Time

Finally the effect of the layer depth on the rate of consolidation of the raft was examined. The problem chosen was a raft of stiffness  $K = 1.0$  which is loaded by a uniform loading  $q_A$  applied at time  $t = 0^+$  and thereafter held constant. The base of the layer was chosen to be rough and rigid.

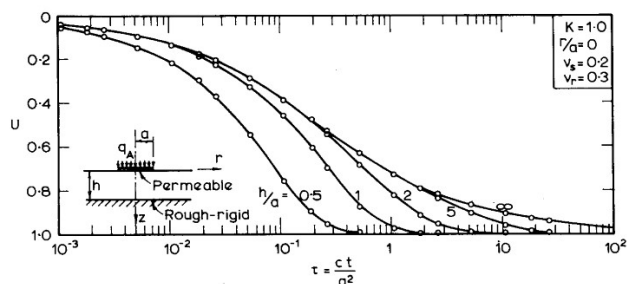


Fig. 7 Degree of Consolidation for Soil Layers of Different Thicknesses - Circular Raft

Results are presented in Figure 7 for various layer depths  $h/a = 0.5, 1, 2, 5, \infty$ . Degree of consolidation  $U$  is plotted against time factor in this figure where

$$U = \frac{w(0, t) - w(0, 0)}{w(0, \infty) - w(0, 0)} \quad (13)$$

As would be expected the deeper layers do not consolidate as rapidly as the more shallow layers.

In order to calculate actual deflections at the centre of the raft, the initial and final values need to be inserted into (13). Values may be calculated from the results presented by Brown (1972), provided the correct initial and final modulus and Poisson's ratio are used.

#### 4. CONCLUSIONS

A method has been presented to enable the settlements of circular rafts to be calculated at any time during consolidation. Using the method, differential deflections and moments in the raft may also be computed at any time.

The theory and results presented have application in the prediction of the rate of settlement of any circular raft type foundation. For more complicated or time dependent loadings or the inclusion of more complicated structures (i.e. the walls of tanks, silos etc.) the theory presented here may be easily extended.

One application of the results may be to plate load testing. It may be possible to backfigure the value of  $c$  (or  $c_v$ ) for a layer of soil if field data for the time-deflection curve of the plate is known. This would involve fitting the experimental curve to the theoretical curve in much the same way as is done in the standard "root" time and "log" time methods of obtaining  $c_v$  from the oedometer test.

#### 5. REFERENCES

- BOOKER, J.R. (1974). The Consolidation of a Finite Layer Subject to Surface Loading, Int. Jnl. Solids and Structs., Vol.10, pp.1053-1065.
- BOOKER, J.R. and SMALL, J.C. (1983). The Time Deflection Behaviour of a Circular Raft of Finite Flexibility on a Deep Clay Layer. School of Civil and Mining Eng. Research Report R434, University of Sydney.
- BOROWICKA, H. (1936). Influence of Rigidity of a Circular Foundation Slab on the Distribution of Pressures over the Contact Surface, Proc. First Int. Conf. Soil Mech., p.144.
- BROWN, P.T. (1969a). Numerical Analyses of Uniformly Loaded Circular Rafts on Elastic Layers of Finite Depth, Geotechnique, Vol.19, No.2, pp.301-306.
- BROWN, P.T. (1969b). Numerical Analyses of Uniformly Loaded Circular Rafts on Deep Elastic Foundations, Geotechnique, Vol.19, No.3, pp.399-404.
- BROWN, P.T. (1972). The Analysis of Rafts on Clay, PhD Thesis, Dept of Civil Engineering, University of Sydney.
- DAVIS, E.H. and POULOS, H.G. (1963). Triaxial Testing and Three Dimensional Settlement Analysis, Proc. 4th ANZ Conf. on Soil Mech. Found. Eng., pp.233-243.
- DAVIS, E.H. and POULOS, H.G. (1972). Rate of Settlement under Two and Three Dimensional Conditions, Geotechnique, Vol.22, No.1, pp.95-114.
- GIBSON, R.E. and McNAMEE, J. (1963). A Three Dimensional Problem of the Consolidation of a Semi-infinite Clay Stratum, Quart. Jnl. Mech. Appl. Math., Vol.XVI, Pt.2, pp.115-127.
- GIBSON, R.E., SCHIFFMAN, R.L. and PU, S.L. (1970). Plane Strain and Axially Symmetric Consolidation of a Clay Layer on a Smooth Impervious Base, Quart. Jnl. Mech. Appl. Math., Vol.XXIII, Pt.4, pp.505-519.
- HABEL, A. (1937). Die auf dem elastisch-isotropen Halbraum aufruheude zentral-symmetrisch belastete elastische Kreisplatte, Bauingenieur, Vol.18, No.15/16, p.188.
- HOLMBERG, A. (1946). Cirkulara plattor med jamnt fordelad last pa elastiskt underlag, Betong, No.1, p.7.
- McNAMEE, J. and GIBSON, R.E. (1960). Displacement Functions and Linear Transforms Applied to Diffusion Through Porous Elastic Media, Quart. Jnl. Mech. Appl. Math., Vol.XIII, Pt.1, pp.98-111.
- TALBOT, A. (1979). The Accurate Numerical Inversion of Laplace Transforms, Jnl. Inst. Maths. Applics., Vol.23, pp.97-120.
- TERZAGHI, K. (1925). Erdbaumechanik auf Boden physikalischer Grundlage, F. Deuticke, Vienna.
- TIMOSHENKO, S.P. and WOINOWSKY-KRIEGER, S. (1959). Theory of Plates and Shells, McGraw Hill Book Co., New York.

#### APPENDIX A

It may be shown by using the theory of McNamee and Gibson (1960) that the surface displacement  $w(r,t)$  of a layer of soil is given by the expression

$$\bar{w}_h = \rho(\alpha, s) \frac{\bar{q}_h}{2G} \quad (A1)$$

where the superior bar denotes a Laplace transform and the subscript h denotes a Hankel transform i.e.

$$\bar{w}_h = \int_0^\infty \left( \int_0^\infty r w(r,t) J_0(\alpha r) dr \right) e^{-st} dt$$

The value  $\bar{q}_h$  is derived from the loading applied to the soil layer which in this case is the contact stress  $q_c(r,t)$ .

Expressions for  $\rho(\alpha, s)$  are given below:

I ROUGH BASE

$$\rho(\alpha, s) = -1/\alpha\Omega(\alpha) \quad (A2)$$

$$\text{where } \Omega(\alpha) = (I_1 + I_2 f(\alpha) - \alpha \left( \frac{\alpha c}{ns} - 1 \right))$$

$$\text{and } I_1 = \frac{\alpha c}{ns} \left[ \frac{(\alpha^2 + \beta^2)}{\beta} T_\alpha T_\beta - \frac{\alpha T S}{C_\alpha} + \frac{\alpha}{C_\beta C_\alpha} \right] - \alpha h T_\alpha$$

$$I_2 = \frac{\alpha c}{ns} \left[ \frac{\alpha^2}{\beta} T - \frac{\alpha S}{C_\beta} \right] - \alpha h$$

$$f(\alpha) = \frac{\frac{\alpha c}{ns} \left( \frac{\alpha T_\alpha C_\alpha}{C_\beta} - \alpha T_\alpha - \beta T_\beta \right) + I_1 T_\alpha + \alpha h - T_\alpha}{\frac{\alpha c}{ns} \left( \alpha \frac{C_\alpha}{C_\beta} - \alpha \right) + I_2 T_\alpha + \alpha h T_\alpha - 1}$$

$$\begin{aligned} \text{and } C_\alpha &= \cosh(\alpha h) \\ C_\beta &= \cosh(\beta h) \\ S_\alpha &= \sinh(\alpha h) \end{aligned}$$

$$\begin{aligned} T_\alpha &= \tanh(\alpha h) \\ T_\beta &= \tanh(\beta h) \end{aligned}$$

$$\eta = \frac{(1 - \nu_s)}{(1 - 2\nu_s)}$$

## II SMOOTH BASE

$$\rho(\alpha, s) = -1/\alpha\Omega(\alpha) \quad (\text{A3})$$

where

$$\Omega(\alpha) = \left[ \frac{\alpha c}{\eta s} (\alpha - \beta) + \frac{T_\beta}{T_\alpha} + \frac{h}{S_\alpha C_\alpha} + 1 \right]$$

In both the rough and smooth base cases the expressions for large  $h$  (or equivalently large  $\alpha$ ) tend to the same expression.

$$\rho(\alpha, s) = -1/\alpha\Omega(\alpha) \quad (\text{A4})$$

$$\text{where } \Omega(\alpha) = (\alpha c/\eta s)(\alpha - \beta) + 1$$

which is the solution for the infinitely deep layer of soil.

In the above expressions

$$c = 2G \frac{(1 - \nu_s) k}{(1 - 2\nu_s) \gamma_w}$$

$G$  is the shear modulus of the soil  
 $\nu_s$  is the Poisson's ratio of the soil  
 $k/\gamma_w$  is the permeability of the soil per unit weight of water  
 $c$  is therefore indential to the one dimensional coefficient of consolidation.

Because of the definition of  $q_c(r, t)$  given in Eq. 1 we may write

$$\bar{q}_h = \sum_{n=1}^N \bar{F}_n \phi_n(\alpha) \quad (\text{A5})$$

where

$$\phi_n(\alpha) = \int_0^a r \phi_n(r) J_0(\alpha r) dr$$

and evaluating this integral gives the expression

$$\phi_n(\alpha) = \frac{a^2 \Gamma(n+1) J_{n+1}(\alpha a)}{2(\alpha a/2)^{n+1}} \quad n = 1, 2, 3 \dots N-1$$

$$\phi_N(\alpha) = \frac{a^2 \sin(\alpha a)}{(\alpha a)}$$

$$n = N = -\frac{1}{2}$$

Substituting for  $\bar{q}_h$  in Eq. B1 we obtain

$$\bar{w} = \frac{\rho(\alpha, s)}{2G} \sum_{n=1}^N \bar{F}_n \phi_n(\alpha) \quad (\text{A6})$$

The application of an inverse Hankel transform gives the required solution for the vertical displacement  $w$ .

$$w = \frac{1}{2G} \int_0^\infty \alpha \rho(\alpha, s) \sum_{n=1}^\infty \bar{F}_n \phi_n(\alpha) J_0(\alpha r) d\alpha \quad (\text{A7})$$

The appropriate value of  $\rho(\alpha, s)$  must be used according to whether the base of the layer is rough or smooth.